JOURNAL OF APPLIED ELECTROCHEMISTRY 12 (1982) 487–496

Alternating current impedance studies on oxide films in metal/oxide/electrolyte systems: a modified approach

R. SRINIVASAN, C. S. C. BOSE

Department of Chemistry, Indian Institute of Technology, Powai, Bombay 400076, India

Received 8 December 1981

The accurate determination of the impedance of oxide films in metal/oxide/electrolyte systems is shown to be possible through a modified procedure. The film impedance thus determined is found to be quite different from the measured cell impedance for anodic aluminium oxide formed on pure aluminium. The computed values of tan δ and conductivity are found to be in agreement with the values reported earlier for anodic and thermal oxides.

1. Introduction

Many electrochemical methods have been employed to study the nature of metal/oxide/electrolyte interfaces. In such systems, the oxide layer plays an important role in both the uniform and local corrosion of metals [1, 2]. Among the electrochemical techniques used in such studies, potentiodynamic [1], impedance techniques based on pulse-transients [3, 4] and a.c. signals [5–9], are quite common. Of these, the low voltage a.c. impedance methods (normally less than 5 mV) are useful wherever any kind of modification of the nature of the oxide is undesirable. The impedance is analysed by taking electrical equivalent analogues in terms of resistance, capacitance and inductance in series and/or in parallel.

Figure 1 shows a simple representation of a metal/oxide/electrolyte system.

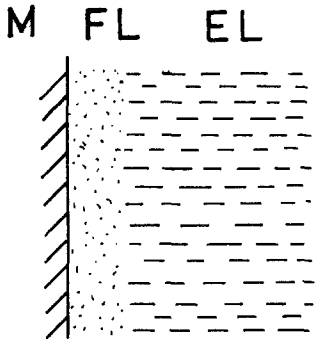

Fig. 1. A simple representation of the metal/oxide/electrolyte system: M, metal; FL, oxide film; EL, Electrolyte.

Electrical impedance due to the oxide film, Z_{fl}, and the oxide electrolyte interface, Z_r, and the resistance due to the electrolyte, R_Ω, can all be taken to be in series with each other. Thus, the impedance of the simplest reasonable model for the metal/oxide/electrolyte system is a uniform transmission line type as depicted in Fig. 2a. Its net impedance, Z_t, can be given as

$$Z_t = Z_{fl} + Z_r + R_\Omega. \quad (1)$$

The impedance, Z_{fl}, can be represented in terms of a simple equivalent circuit comprising of a resistance, R_{fl}, and a capacitance, C_{fl}, taken in series. In principle however this might be expanded further into more complex analogues in order to analyse the structure and properties of the film. Similarly, the impedance, Z_r, can be represented in terms of an equivalent series resistance, R_r, and capacitance, C_r. Together they represent components of, for example, double layer capacitance and various other impedances due to faradaic reactions, non-faradaic reactions and mass transfer.

Figure 2b represents Z_{fl}, Z_r and R_Ω in terms of electrical equivalent circuits.

Experimental determination of the impedance of a metal/oxide/electrolyte system normally yields Z_t. Separating the individual values of Z_{fl}, Z_r and R_Ω from the measured impedance is apparently difficult, although, in principle, a separate calculation of the solution resistance, R_Ω, is possible from a knowledge of its specific resistance and electrode geometry.

0021–891X/82/040487–10$03.70/0

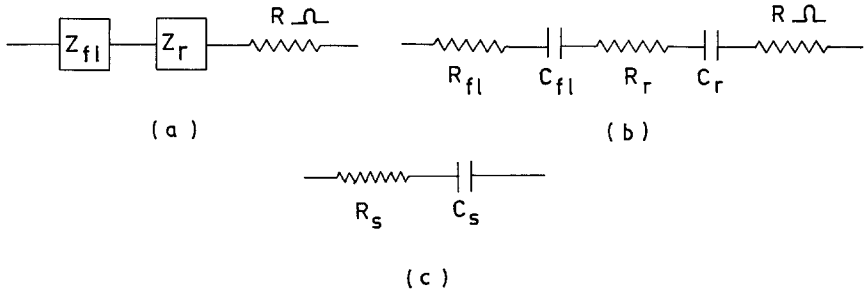

Fig. 2. (a) Transmission line analogue of the impedance of the system in Fig. 1. (b) Series equivalent circuit representation of the impedances Z_{fl} and Z_r and the solution resistance R_Ω in Fig. 2a. (c) A simple series equivalent circuit representation of Fig. 2b.

However, most of the earlier workers [5, 6, 10] assumed that the solution resistance and the oxide/electrolyte interfacial impedance was negligible in relation to the oxide film impedance. Such an assumption regarding R_Ω may hold good if the electrolyte is highly conducting and the distance between the electrodes is kept very small. As for Z_r, its relatively small value can not be justified. On the other hand, it is well known that the double layer capacitance of any electrode depends upon its potential [11], and no knowledge of this capacitance exists for oxide-covered metal electrodes. Also, no adequate knowledge exists about the faradaic and non-faradaic impedances due to oxide/electrolyte interfaces.

To overcome these difficulties, Wood and co-workers [7, 12, 13], and Libsch and Devereux [14] have made use of a dummy platinum electrode in place of oxide-covered (aluminium) electrodes. They have taken the measured impedance of such a cell as equal to the sum of Z_r plus R_Ω of the cell with the aluminium electrode and calculated Z_{fl}, the impedance due to the oxide film.

Again this is a questionable practice in that the impedance due to double layer capacitance, faradaic and non-faradaic reactions and due to mass transfer are taken to be the same on the two electrodes [15]. As a result, this kind of correction can lead to erroneous conclusions with regard to the properties of the oxide film.

In the present work, a modified approach is proposed in order to determine the oxide film impedance of metal/oxide/electrolyte systems without having to resort to the assumptions discussed above. The validity of the proposed approach is demonstrated for anodic aluminium oxide formed using two different electrolytes, namely, ammonium tartrate (known to form barrier-type films) and sulphuric acid (known to produce porous films at high anodizing voltages, but barrier films at low voltages of formation [10]).

2. Proposed modified approach

The circuit elements of the oxide electrode shown in Fig. 2b may also be represented in terms of a resistance and capacitance which are in series (R_s–C_s), as seen in Fig. 2c.

It follows from circuit theory that the impedance vector $\mathbf{Z}_t$ for the equivalent circuit in Fig. 2c is given by

$$\mathbf{Z}_t = R_s - \frac{j}{\omega C_s} \tag{2}$$

where $j = (-1)^{1/2}$, $\omega = 2\pi f$ and f is the frequency in hertz.

Similarly the impedance vectors $\mathbf{Z}_{fl}$ and $\mathbf{Z}_r$ (Fig. 2a and b) are given by

$$\mathbf{Z}_{fl} = R_{fl} - \frac{j}{\omega C_{fl}} \tag{3}$$

and

$$\mathbf{Z}_r = R_r - \frac{j}{\omega C_r}. \tag{4}$$

It should be pointed out here that for the given model (Fig. 1), the film impedance, Z_{fl}, depends upon the thickness, x and the geometric area, A, of the oxide. In contrast the oxide/electrolyte interfacial impedance, Z_r, is independent of x and A, but depends upon the true surface area, A'. Thus Equations 3 and 4 should be modified accordingly. Further, between Equations 1 and 2

the real and imaginary terms can be separated to give

$$R_s = \frac{x}{A}R_\sigma + \frac{1}{A'}R'_r + R_\Omega \quad (5)$$

and

$$\frac{1}{\omega C_s} = \frac{x}{\omega A C_\sigma} + \frac{1}{\omega A' C'_r} \quad (6)$$

where R_σ and C_σ are the equivalent series resistance and capacitance of the oxide film of unit thickness and geometric area, and R'_r and C'_r are the corresponding terms for the oxide/electrolyte interface with unit true surface area.

Differentiating Equations 5 and 6 with respect to x gives,

$$\frac{d(R_s)}{dx} = \frac{R_\sigma}{A} \quad (7)$$

and

$$\frac{d(1/\omega C_s)}{dx} = \frac{1}{\omega A C_\sigma}. \quad (8)$$

From Equations 7 and 8, R_σ and C_σ can be determined at any given value of ω.

In practice, R_s and C_s can be determined experimentally at various oxide film thicknesses in any electrolyte (preferably the one which reacts least with the film) at any value of ω. From Equations 5 and 6, the slopes of plots of R_s versus x and C_s versus x should give the values of Equations 7 and 8, respectively. It can also be seen that the intercepts of these plots should give information about Z_r. However, analysis of Z_r by itself is likely to be quite involved and, therefore, is not included in the present study.

3. Experimental details

3.1. *Test specimens*

Zone refined 99.999% pure polycrystalline aluminium rod was masked with a push-fit Teflon holder, exposing a disc-like surface of geometric area 1.96×10^{-5} m^2. The other end of the rod was plated with zinc followed by copper and used for electrical contacts. (Such a procedure ensured a perfect ohmic contact.) The test specimen was then polished using an alumina suspension on a rotating table. The surface was further treated according to a procedure prescribed by Norman [16], which leaves an initial oxide film of reproducible thickness (30 Å). It was anodized thus at 6 V for 1 min in 0.5 mol dm^{-3} ammonium tartrate (pH = 6) at 25 ± 1° C followed by etching in 48% HF for 10 to 15 s. This anodizing and etching cycle was repeated three times. The electrode was anodized further at different voltages prior to impedance measurements, either in ammonium tartrate or sulphuric acid (see Section 3.5).

3.2. *Test solutions*

The choice of the test electrolyte for impedance measurements was made so that the ions were compatible with those of the anodizing electrolyte. Thus, 1 mol dm^{-3} sodium sulphate was used after anodizing in sulphuric acid. With anodizing in ammonium tartrate the same solution was used as the test solution. Both test solutions were adjusted to pH 6 where the aluminium oxide is known to be most stable [6, 7, 10].

All the solutions were prepared from reagent grade salts recrystallized from double-distilled water. Sulphuric acid used for anodizing was of Analar grade and was redistilled under vacuum.

The solutions were saturated with nitrogen for 1 h in a separate 100 cm^3 glass cell and transferred to the electrochemical cell under nitrogen for impedance measurements. The temperature of the solutions was maintained at 25 ± 1° C.

3.3. *Electrochemical cell*

An all glass cell with a 100 cm^3 capacity was used (Fig. 3). A platinized platinum electrode in the form of a 5 mm diameter disc was held in a Teflon holder and used as a counter electrode. The Teflon holders of both the test and counter electrodes were machined to match the glass joints, which were fused diametrically opposite and concentric to each other. This helped in keeping the distance between the electrodes constant every time these were mounted onto the cell.

3.4. *Test circuit*

The bridge adopted for the present work was essentially of the Wein type with slight modifications (Fig. 4). The oscillator was connected to the bridge through a shielded transformer, a high leakage-resistance capacitor and a potentiostat. Two non-inductive resistances were matched to

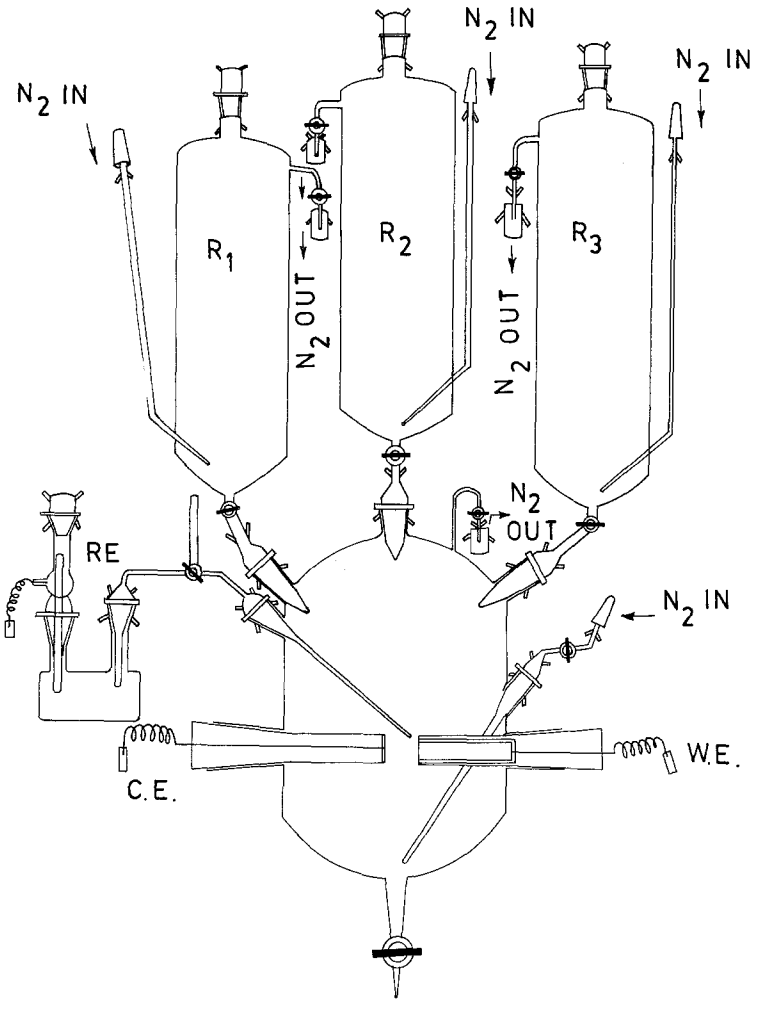

Fig. 3. Electrochemical cell used for impedance measurements. WE, 99.999% pure aluminium test electrode; CE, platinized platinum counter electrode; RE, reference electrode with a luggin bridge; R_1, R_2, R_3, reserviors for nitrogen saturated anodizing electrolyte, test electrolyte and double-distilled water, respectively.

give identical values and used as ratio arms. A decade capacitance box and a decade resistance box coupled in series were used in the balancing arm. A vector lock-in amplifier with a simultaneous read-out of in-phase and quadrature components was used as null detector. The balancing points of the bridge were connected to it in the floating mode. A constant 1 V output from the oscillator, in phase with the signal applied across the bridge, was fed to its reference. The braids of the sheilded cables used as leads and the other points of the bridge required to be earthed were earthed through the lock-in amplifier earth.

The bridge circuit was first tested with standard resistances and capacitances. Its accuracy was within a 1% error limit at frequencies above 10^3 Hz. But at lower frequencies this limit gradually increased to a maximum of 10%, which was possibly due to the resistance and capacitance in the balancing arm being in series (which, however, had to be adopted in order to avoid closed circuit d.c. currents which might otherwise exist due to the natural potential difference between the aluminium and platinum electrodes).

3.5. *Procedure*

The anodizing medium (ammonium tartrate or sulphuric acid) was deaerated and transferred to the cell under nitrogen. The test electrode was then anodized with a voltage pulse of desired magnitude for 1 min.

In the case of ammonium tartrate anodizing, impedance measurements were started within 5 min of the time of anodizing. However, in the case of sulphuric acid anodizing, the solution was

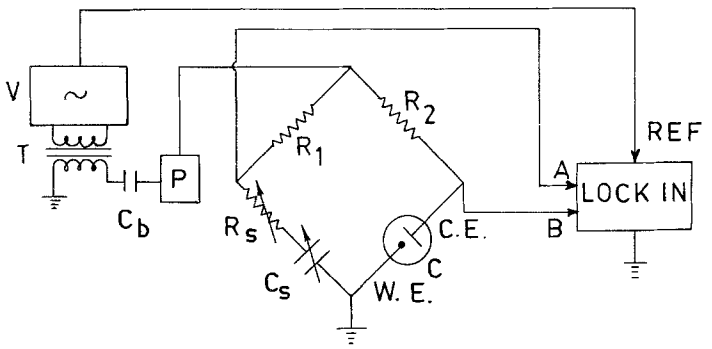

Fig. 4. The a.c. impedance bridge: V, oscillator; T, shielded transformer; Cb, high leakage-restance 10 μF polystyrene capacitor; P, potentiostat; R_1, R_2, inductance free resistances of 99.97 Ω each; R_S, low-inductance decade resistance box; range × 0.01 to × 1000 Ω with a total resistance 11 111.11 Ω; C_S, shielded decade capacitance box; range × 0.0001 to × 0.1 μF with a total capacity of 11.111 11 μF; C, electrochemical cell; WE, test electrode; CE, counter electrode; LOCK IN, lock-in amplifier (null-detector) (PAR Model 5204); A, B, input to LOCK IN from the balancing points of the bridge; REF, reference input to the LOCK IN from V.

first removed from the cell soon after anodization under nitrogen. Deaerated double-distilled water was immediately flushed into the cell and allowed to flow out in the same way. Deaerated sodium sulphate solution was then pumped into the cell and impedance measurements started within 5 min.

Impedance measurements were carried out in the frequency range 10 to 10^5 Hz using an a.c. potential of less than 1 mV rms across the cell. The range of anodizing voltage covered was from 1 to 40 V. Two experiments were carried out for each anodizing voltage and the average impedance value noted. Measured R_s and C_s values were reproducible within 5% at 2×10^2 Hz and above. At lower frequencies this limit varied between 10 and 20%. It took about 30 min to cover the entire frequency range. At certain voltages, selected at random, the frequency range was covered once in the forward direction (10 to 10^5 Hz) and then in the reverse direction. R_s and C_s values thus measured were stable within a 1% limit.

The thickness of aluminium oxide produced at various voltages during the above study was calculated using the relationship:

$$x = 12.5\,V \times 10^{-10} + x_i \qquad (9)$$

where x_i is the initial thickness of the oxide formed after etching in HF and V is the anodizing voltage.*

This relationship, when transferred to Equations 5 and 6 and differentiated with respect to V, gives

$$\frac{dR_s}{dV} = \frac{12.5R_\sigma}{A} \times 10^{-10} \qquad (10)$$

and

$$\frac{d(1/\omega C_s)}{dV} = \frac{12.5}{\omega A C_\sigma} \times 10^{-10}. \qquad (11)$$

Thus, it was sufficient to measure R_s and C_s at various anodizing voltages in order to determine the R_σ and C_σ values of anodic oxide.

4. Results and discussion

Figure 5 represents the measured R_s values as a function of anodizing voltage for the system: aluminium/aluminium oxide/0.5 mol dm^{-3} ammonium tartrate. A similar plot is shown in Fig. 6, for the same system, for the calculated values of $1/\omega C_s$ using experimentally measured C_s values.†

A reasonable linearity is observed in both cases at all frequencies above 10^3 Hz. However, this is not so below 10^3 Hz, especially at anodizing voltages above 20 V. This may be due to the decreased sensitivity of the bridge at frequencies less than 10^3 Hz (see Section 3.4). Hence, at these frequencies, only R_s and C_s values at 20 V and below were considered for such plots.

* Such a relationship for anodic oxides formed using ammonium tartrate on pure aluminium has been established by Norman [16], using an ellipsometric technique. The same relationship is also known to hold good for sulphuric acid anodizing at low voltages [10].

† R_s and $1/\omega C_s$ behaviour with respect to anodizing voltages were similar in the case of 1 mol dm^{-3} sodium sulphate electrolyte also and hence not separately shown. The frequency range covered with sodium sulphate was from 80 to 10^4 Hz only.

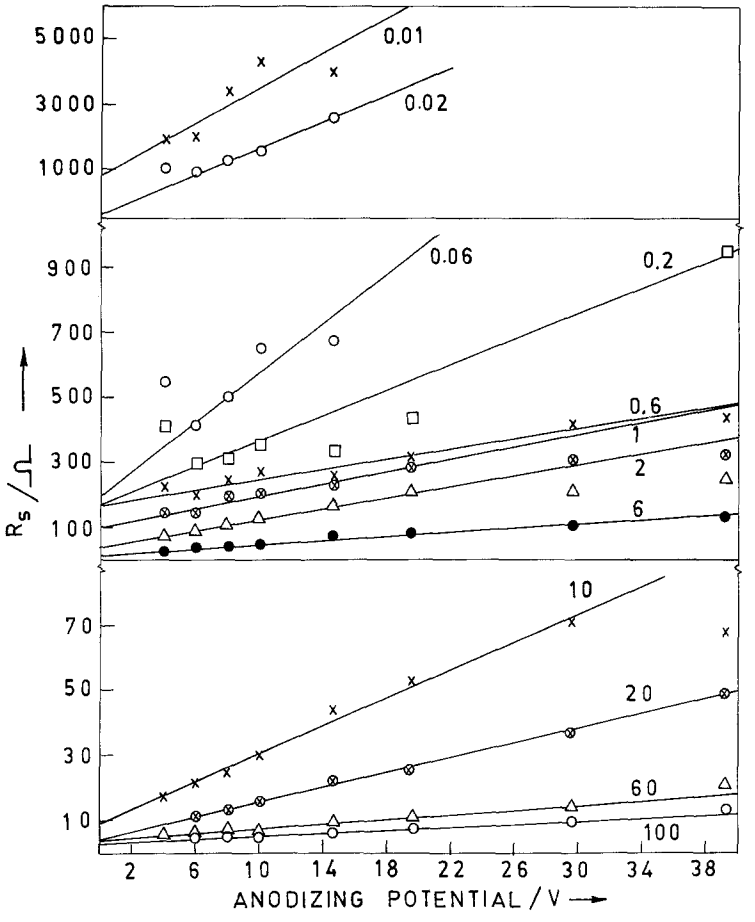

Fig. 5. Dependence of the measured series resistance (R_s) on anodizing voltage (V) for the system: aluminium/aluminium oxide/0.5 mol dm^{-3} ammonium tartrate. The numbers on the curves represent the frequency of measurements in kHz.

The slopes of the above plots were determined by a least squares curve fitting method. Making use of these data, the impedance values for a film of 1 m^2 geometric area and 130 x 10^{-10} m thickness were computed. These impedance plots are shown in Fig. 7 for the two test electrolytes. The experimentally measured cell impedances with the electrode anodized at 8 V (corresponding to a total film thickness of 130 Å) are also shown in the same figure in order to bring out their contrast with the respective oxide film impedances (computed as above).

Figures 8 and 9 represent the computed values of tan δ (tan $\delta = \omega R_{fl} C_{fl}$) and a.c. conductivity, $\sigma(\sigma = \omega\epsilon''\epsilon_0 \simeq \omega\epsilon_0 \tan\delta$, where ϵ_0 is the permitivity in vacuum and ϵ'' is the imaginary part of the complex dielectric constant) for the oxide films over the range of frequencies employed.

The measured cell impedances (Fig. 7) are linear upto 400 Hz and become curved at higher frequencies. Normally, this could have been justified as the expected behaviour of cells with a test electrode covered with a passive film [5, 17].

The computed impedance of the oxide film shows an essentially similar behaviour. However, there are important differences. Thus, the magnitude of the impedance is significantly different from the cell impedance at almost all frequencies. Furthermore, although the impedance plot is linear upto 400 Hz, which is the case with the cell impedance, the curved behaviour begins only at frequencies above 3 x 10^3 Hz. The intermediate frequency region is marked by a sharp change in the imaginary component of the impedance.

Table 1 shows the values of the impedance (taken as $|Z| = (|Z'|^2 + |Z''|^2)^{1/2}$ of the oxide films, and those of the cell at various frequencies. Also included are the values of the impedance due to the oxide/electrolyte interface, computed from the cell impedance after correcting for the oxide

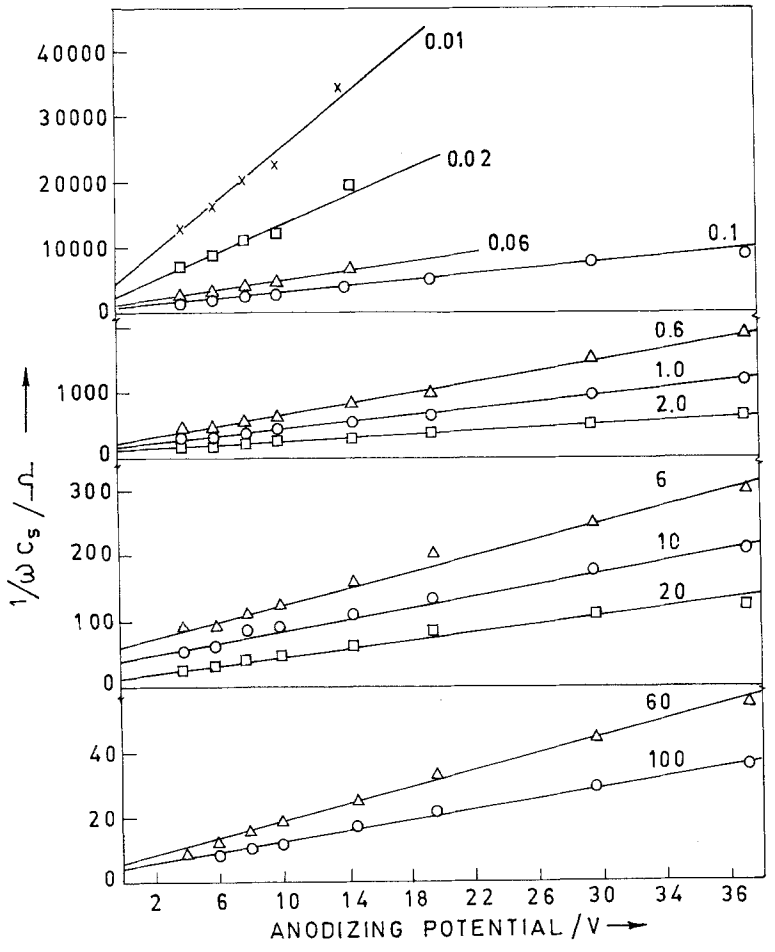

Fig. 6. Dependence of the measured $1/\omega C_s$ on anodizing voltage (V) for the system: aluminium/aluminium oxide/ 0.5 mol dm^{-3} ammonium tartrate. The numbers on the curves represent frequency of measurements in kHz.

film impedance and electrolyte resistance (obtained by extrapolating the cell impedance in Fig. 7 to infinite frequency).

It may be noted from Table 1 that $|Z_t|$ is significantly larger than $|Z_{fl}|$ for both the test electrolytes. $|Z_r|$ values are found to be comparable with those of $|Z_{fl}|$. Thus, if the oxide film impedance was to be determined from a single measurement of cell impedance, then the correction required to be applied for oxide/electrolyte impedance, as well as the electrolyte resistance, are found to be quite large. Thus, any assumption that $|Z_r| \ll |Z_{fl}|$, or that $|Z_r|$ of any other oxide free metal/electrolyte system is equal to that of the oxide/electrolyte interfacial impedance, can lead one to erroneous conclusions.

The behaviour of the oxide film impedance observed is also in general agreement with the behaviour of aluminium/aluminium oxide systems (measured in the absence of any electrolyte using gold or copper as the counter electrode) reported in literature [18, 19].

In the present study, tan δ for aluminium oxide formed by ammonium tartrate anodization shows a maximum at about 2.5×10^3 Hz, and is found to be frequency independent below 400 Hz (Fig. 8).

Three regions of conductivity are observed with distinct changes occurring at 2.5×10^3 and 400 Hz, respectively (denoted by Regions I, II and III in Fig. 9). Region I obeys a linear law ($\sigma \propto f$), and Region II a square law ($\sigma \propto f^2$). In Region III, the law is $\sigma \propto f^{0.7}$.

Essentially similar behaviour is observed for films formed in sulphuric acid.

The increase of conductivity with frequency may be explained on the basis of a conduction mechanism proposed by Smyth [20] and Pollak [21]. Thus, in Region I, it is the hopping of elec-

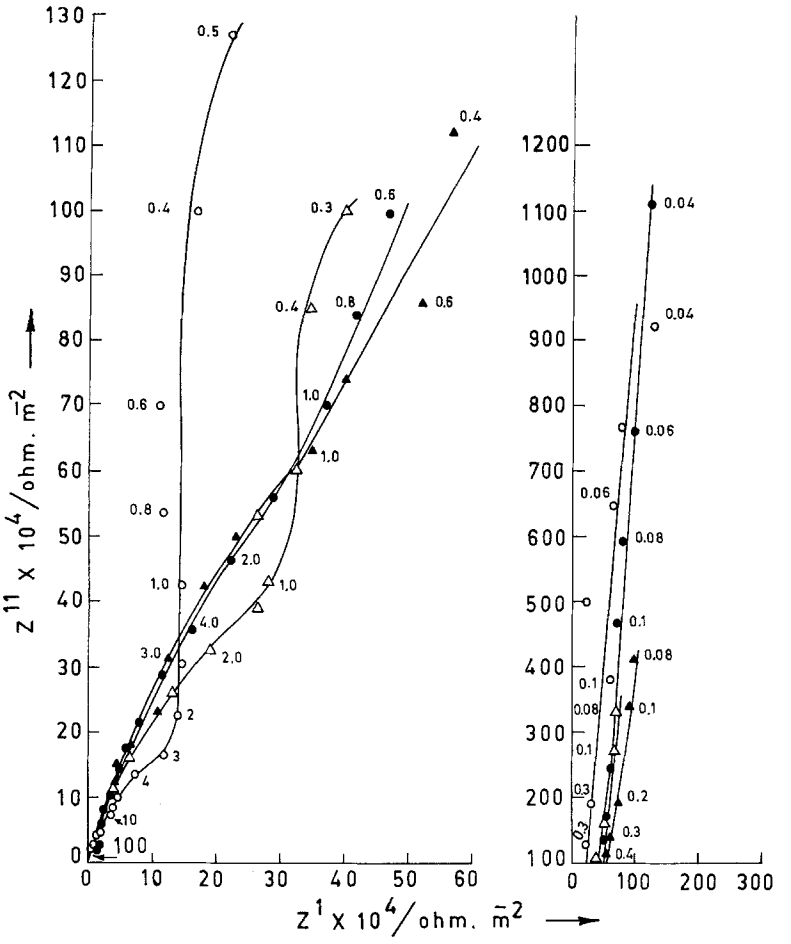

Fig. 7. Impedance plots of 130 Å thick aluminium oxide films and electrochemical cells with anodized (at 8 V) aluminium electrodes. The numbers on the curves represent frequency in kHz. Z' is the real part (equal to R_{fl} for the oxide films and R_s for the cells). Z'' is the imaginary part (equal to $1/\omega C_{fl}$ for the oxide films and $1/\omega C_s$ for the cells). ○–○ Computed values for the oxide film in Al/oxide/0.5 mol dm^{-3} ammonium tartrate system; ●–● calculated from the measured R_s and C_s values for the cell of the same system; △–△ computed values for the oxide film in Al/oxide/1 mol dm^{-3} Na_2SO_4 system; ▲–▲ calculated from the measured R_s and C_s values for the cell of the same system.

trons between pairs of sites (caused by vacancies etc.) that aids conduction. The ability of electrons to hop between site pairs with decreasing separation increases with frequency (Region II) and tends to reach a saturation value at much higher frequencies (Region III and above). The contribution to conduction by quantum mechanical tunnelling of electrons cannot be totally ruled out,

Table 1. Magnitudes of impedance values, calculated as $|Z| = (Z'^2 + Z''^2)^{1/2}$ *for the oxide films, the electrochemical cells and the oxide/electrolyte interfaces*

Frequency (kHz)	*Computed values for 130 Å thick* Al_2O_3 *film* (Z_{fl}) ($\times 10^{+4}\ \Omega\ m^{-2}$)		*Measured values of the electrochemical cell* (Z_t) ($\times 10^{+4}\ \Omega\ m^{-2}$)		*Computed value for oxide/electrolyte interface* (Z_r) ($\times 10^{+4}\ \Omega\ m^{-2}$)	
	0.5 mol dm^{-3} *ammonium tartrate*	*1 mol* dm^{-3} Na_2SO_4	*0.5 mol* dm^{-3} *ammonium tartrate*	*1 mol* dm^{-3} Na_2SO_4	*0.5 mol* dm^{-3} *ammonium tartrate*	*1 mol* dm^{-3} Na_2SO_4
60	2.10	–	3.34	–	1.10	–
10	7.97	11.74	15.49	12.87	7.50	1.56
1	44.90	51.27	79.54	72.66	35.33	21.29
0.1	387.40	276.20	472.40	352.80	84.90	84.70
0.01	3159.90	–	4073.10	–	931.15	–

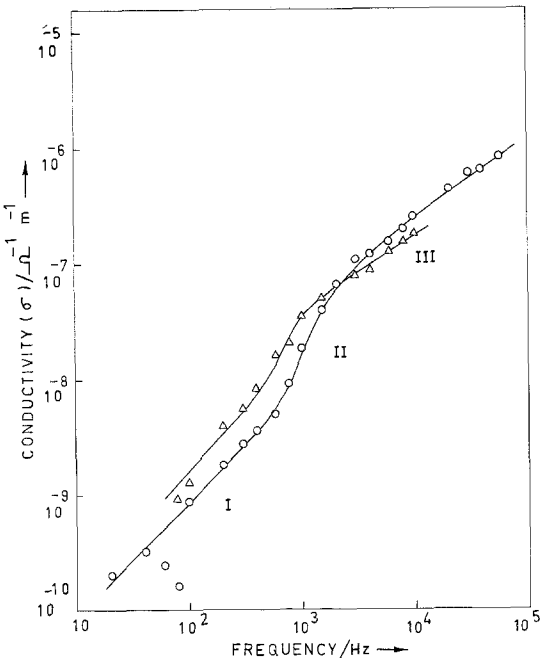

Fig. 8. Dependence of tan δ on log of frequency as computed for 130 Å thick oxide film: o–o For Al/aluminium oxide/0.5 mol dm^{-3} ammonium tartrate; △–△ for Al/aluminium oxide/1 mol dm^{-3} sodium sulphate.

otherwise the properties of such films which are known to sustain cathodic reduction reactions at the oxide/electrolyte interface under d.c. polarization conditions could not be explained [22].

A thorough understanding of the exact mechanism of conduction requires a more detailed study. However, there is no need to invoke the possibility

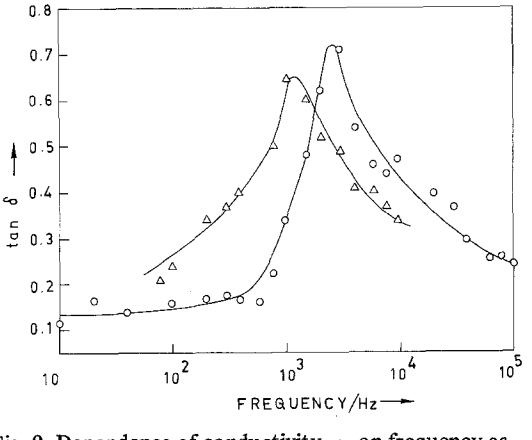

Fig. 9. Dependence of conductivity, σ, on frequency as computed for 130 Å thick oxide film: o–o For Al/aluminium oxide/0.5 mol dm^{-3} ammonium tartrate; △–△ for Al/aluminium oxide 1 mol dm^{-3} sodium sulphate.

of porosity in the anodic film to explain the impedance behaviour. The presence of pores would have considerably reduced the chances of linear behaviour for R_s and $1/\omega C_s$ with respect to the anodizing voltage (see Figs. 5 and 6). In addition, transmission electron microscopic studies have shown that the films formed under analogous conditions are either free from pores [14] or that the pore diameter is very small (< 200 Å) with a very small ratio of pore area to the total area of the film [13] (10^{-2}–10^{-3}). Such films are also known to withstand an excess gas pressure of 0.14 atm without allowing the gas to diffuse through them [23].

It should also be noted that the behaviour of tan δ and conductivity depends upon the type of aluminium oxide used. Thermal oxides [18] are known to behave very differently from anodic oxides [19]. In addition, the history of specimen preparation also seems to play a crucial role; thus, anodic aluminium oxide films dried under vacuum and exposed to controlled quantities of oxygen are known to show changes in their tan δ values [24].

Acknowledgements

The authors would like to thank Professor Hira Lal and Dr H. S. Gadiyar, Metallurgy Division, BARC, Bombay, for useful discussions.

References

[1] G. Bombara, *Corros. Sci.* **19** (1979) 991.
[2] T. B. Grimly, 'Corrosion', Vol. 1 (edited by L. L. Shrier), George Newnes Ltd, London (1963) p. 1.152.
[3] J. J. McMullen and N. Hackerman, *J. Electrochem. Soc.* **106** (1959) 341.
[4] R. J. Brood and N. Hackerman, *J. Electrochem. Soc.* **104** (1957) 704.
[5] I. Epelboin and M. Keddam, *Proc 3rd Int. Congr. on Metallic Corros.*, Vol. 1, MIR Publications, Moscow (1969) p. 110.
[6] M. A. Heine and M. J. Pryor, *J. Electrochem. Soc.* **114** (1967) 1001 (see also the other works of M. J. Proyor and co-workers given in this reference).
[7] J. A. Richardson and G. C. Wood, *J. Electrochem. Soc.* **120** (1973) 193 (see also the other works of G. C. Wood and co-workers given in this reference).
[8] R. D. Armstrong and A. C. Coates, *Corros. Sci.* **16** (1976) 423.
[9] D. D. Macdonald, 'Transient Techniques in Electrochemistry', Plenum Press, New York (1977) p. 273.

[10] J. W. Diggle, T. C. Downie and C. W. Goulding, *Chem. Rev.* 69 (1969) 365.
[11] P. Delahay, 'Double layer and Electrode Kinetics', Interscience Publishers, New York (1965) p. 28.
[12] J. A. Richardson, G. C. Wood and A. J. Breen, *Thin Solid Films* **16** (1973) 81.
[13] J. A. Richardson, G. C. Wood and W. H. Sutton, *Thin Solid Films* **16** (1973) 99.
[14] T. A. Libsch and O. F. Devereux, *J. Electrochem. Soc.* **121** (1974) 400.
[15] K. J. Vetter, 'Electrochemical Kinetics', Academic Press, New York (1967) p. 455.
[16] J. E. Norman, *Corros. Sci.* 17 (1977) 39.
[17] D. Schuhmann, *J. Electroanal. Chem.* **17** (1968) 45.
[18] H. Birey, *J. Appl. Phys.* 49 (1978) 2898.
[19] F. Argall and A. K. Jonschar, *Thin Solid Films* **2** (1968) 185.
[20] D. M. Smyth in 'Oxides and Oxide Films', Vol. 2, (edited by J. W. Diggle) Marcel Dekker, New York (1973) p. 148.
[21] M. Pollak, *Phys. Rev.* 138A (1965) 1822.
[22] A. K. Vijh, in 'Oxides and Oxide Films', Vol. 2 (edited by J. W. Diggle) Marcel Dekker, New York (1973) p. 70.
[23] P. F. Schmidt, F. Huber and R. F. Schwarz, *Phys. Chem. Sol.* 15 (1960) 270.
[24] J. A. Aboof, *J. Electrochem. Soc.* **114** (1967) 948.